The chemical composition and manufacturing technology of glass beads excavated from the Hetian Bizili site, Xinjiang

Dong Wang
Northwest University
Rui Wen (rwen80@163.com)
https://orcid.org/0000-0003-0094-1962
Xingjun Hu
Xinjiang Institute of Cultural Relics and Archaeology
Wenying Li
Xinjiang Institue of Cultural Relics and Archaeology

Research article

Keywords: glass eye beads, Xinjiang, the Silk Road, Bizili site

Posted Date: June 15th, 2020

DOI: https://doi.org/10.21203/rs.3.rs-19353/v2

Version of Record: A version of this preprint was published on December 8th, 2020. See the published version at https://doi.org/10.1186/s40494-020-00469-x.

Abstract

The Hetian Bizili site of the Lop County, located in the southern route of the Silk Road in Xinjiang, China, was a trade and cultural hub between the East and the West in ancient times. In 2016, a large number of glass beads were unearthed from the 40 tombs excavated on this site. This study analyzed the chemical composition and manufacturing technology of twelve glass beads from the M5 tomb of the Bizili site by using various analytical techniques such as LA-ICP-AES, EDXRF, Raman Spectrometry, and SR-μCT. The chemical compositions of the beads were all Na 2 O-CaO-SiO 2 , with plant ash and natron as fluxes. The lead antimonite and lead stannate were applied as the opacifying agents. Some of the beads with high contents of aluminum may potentially come from Ancient India. In terms of manufacturing technology, the craftsmen made eyeballs of glass beads in different ways and even applied the same process as Etched Carnelian beads in some beads. This study confirmed that Bizili was an essential place for the interactions between the East and the West and provided the foundation for the spreading of glass beads.

1. Introduction

The Xinjiang Uygur Autonomous Region, located in the northwest of China, has been a vital area of cultural diversity and complexity [1]. Previously, archaeologists focused mainly on the Central Plains of China. Nowadays, Xinjiang has attracted more attention as the findings there could indicate the interactions among various populations in terms of trading goods, technologies, and cultures [2]. A significant number of glass beads in various styles (including faience) have been excavated in the Xinjiang area during the past decades. Based on the published archaeological reports, the earliest faience in China, as early as 1900-1500 B.C, was found in the Adunqiaolu site of Wenquan County, Xinjiang [3]. Besides, the Saensayi site in Urumqi (1700–1500 B.C.), the Tianshanbeilu site (1500–1400 B.C.), and the Ya'er site (1050–910B.C.) in Hami also unearthed faience [4-6]. The earliest glass beads in China were found in Baicheng County and Tacheng County, Xinjiang, dating back to 1100 B.C.–500 B.C. They are all soda-lime glass that was believed to originate from the West. However, some of them show differences in chemical composition, which was probably attributed to the application of local raw materials used by the local craftsmen [7]. The glass beads were spread to China by the ancient nomadic people and all these sites locate in the north of Xinjiang far away from the Silk Road, indicating the cultural exchanges between the East and the West had started before the establishment of the Silk Road. Comparatively, in the south of Xinjiang, the evidence of glass beads in this period was rare until the Han dynasty, since when the amount of evidence has increased sharply. A large number of glass beads have been found in the Shanpula site [8], Niya site [9-10], Jierzankale site [11] and Zhagunluke site [12], with even more than thousand glass beads in the former two sites that distributed along the south of the Silk Road. Meanwhile, the number of glass beads in Northern Xinjiang is relatively small. Such a phenomenon is related the establishment of the Silk Road by Zhang Qian in the Han dynasty. The Han government promoted the trade and cultural exchanges between the Central Plains and Western regions. Also, businessman preferred the south of the Silk Road out of safety concerns that the north of Xinjiang was occupied by the Huns.

The Bizili site situates in the southeast of the Bizili Village, Lop County, in Southern Xinjiang. The Xinjiang Institute of Cultural Relics and Archaeology excavated 40 tombs during the cooperation with road construction in 2016. According to the characteristics of these tombs, the date of the Bizili site was from the Han Dynasty (202 B.C.–220 A.D.) to the Wei and Jin Dynasties (220 A.D.–420 A.D.). These tombs are all pit tombs and can be divided into knife-shaped pit tombs and rectangular pit tombs. The M5 is the largest knife-shaped pit tomb and contains many different bodies. Ninety-seven human bones were found in the M5 filling, with more females than males. Eleven

more human bones were at the bottom of the tomb. Although the tomb was looted and burned sometime before it was excavated, a lot of relics are still preserved, such as potteries, woodwork, pieces of iron, woolen fabrics, and beadwork. Notably, a suet jade pendant was found for the first time in Xinjiang. The dry climate makes it possible to preserve historic relics [13].

In the Han dynasty (202 B.C.–220 A.D.), Bizili belonged to Khotan, a kingdom on the south of the Silk Road. This paper aimed to analyze the chemical composition and manufacturing technology of the glass beads from the Bizili site by using various analytical techniques and to reveal the spread of the ancient glass products and cultural interactions along the Silk Road.

2. Materials And Methods

In this study, ten glass beads excavated from tomb M5 of the Bizili site dating to the Western Han dynasty (202 B.C.–8 A.D.) were selected and tested. Table 1 lists the details of the samples, including the sizes and types, along with the possible origination. The majority of the samples were glass eye beads, a special type with an eye motif on the monochrome surface of the bead [14]. The glass eye bead first appeared during the Eighteenth Dynasty of Egypt, related to the ‘evil eye’ [15]. These unearthed glass beads were generally in good condition with weathering in different degrees on the surfaces. Photographs of some beads are shown in Figure 2.

Table 1 Details of the glass beads from the Bizili site

Sample	Size	Date	Type	Origination
HLB-1	diameter≈1 cm aperture≈0.3–0.5 cm	202 B.C.–8 A.D. (Western Han)	glass eye bead	Bara site
HLB-2	diameter≈1.1 cm aperture≈0.4 cm	202 B.C.–8 A.D. (Western Han)	glass eye bead	Bara site
HLB-3	diameter≈1.3 cm aperture≈0.4 cm	202 B.C.–8 A.D. (Western Han)	glass eye bead	Afghanistan
HLB-4	diameter≈0.5 cm aperture≈0.3 cm	202 B.C.–8 A.D. (Western Han)	glass eye bead	Bara site
HLB-5		202 B.C.–8 A.D. (Western Han)	glass eye bead	Mediterranean and Europe
HLB-6		202 B.C.–8 A.D. (Western Han)	glass eye bead	Mediterranean and Europe
HLB-7		202 B.C.–8 A.D. (Western Han)	monochrome bead	Mediterranean and Europe
HLB-8	diameter≈0.6 cm aperture≈0.2 cm	202 B.C.–8 A.D. (Western Han)	glass eye bead	Bara site
HLB-9		202 B.C.–8 A.D. (Western Han)	glass eye bead	Mediterranean and Europe
HLB-10		202 B.C.–8 A.D. (Western Han)	etched glass bead	Bara site
HLB-11	diameter≈0.35 cm aperture≈0.2 cm	202 B.C.–8 A.D. (Western Han)	monochrome bead	Afghanistan
HLB-12	diameter≈1.4cm aperture≈0.35cm	202 B.C.–8 A.D. (Western Han)	glass bead with pigment	Afghanistan

In this study, we observed typical samples under both optical microscopy and synchrotron radiation microtomography (SR-μCT) to obtain their structural information. Sample surface was cleaned by ethyl alcohol. The optical microscopy observation was carried out in the School of Cultural Heritage, Northwest University. The instrument was a KH-7700 from the HIROX Company, with a MX-5040RZF lens and a metal halogen cold light source. The sample was observed on a 50 times magnification. SR-μCT is a nondestructive 3D imaging technology that can reflect the internal structure of the objects and is suitable for archaeological study. The samples were scanned by synchrotron radiation micro X-ray fluorescence at the Shanghai Synchrotron Radiation Facility,

Shanghai, China. The charge-coupled device detector has a spatial resolution of 5.2 μm. The distance between the detector and samples is 10 cm with the source energy of 28 keV.

Chemical compositions of the samples were analyzed by energy dispersion X-ray fluorescence spectrometry (ED-XRF) and laser ablation inductively-coupled plasma atomic emission spectroscopy (LA-ICP-AES). For better preserved monochrome beads without complex ornaments, the bulk chemistry was determined by ED-XRF at the School of Cultural Heritage, Northwest University. The instrument model is BRUKER ARTAX 400, with a primary beam of 1 mm in diameter. The X-ray energy was 30 kV, the current was 900 μA, and the counting time was 300 seconds. The limit of detection is 0.01. In the experiment, a helium purge was used to allow for the detection of light elements and the standard samples used for calibrations were Corning Glass B, C and D. Table 2 shows the normalized major element contents of the glass standards

The beads decorated with complex patterns (HLB-1, HLB-2, HLB-3, HLB-4, HLB-5, HLB-6, HLB-8, HLB-9, HLB-10 and HLB-12) were analyzed by LA-ICP-AES to obtain accurate chemical compositions of glass beads in different parts. The experiment was carried out in the School of Archaeology and Museology, Peking University. Operation conditions for the LA-ICP-AES system are as follows: 1) RF generator: 40.82 MHz; 2) RF Power: 1.1 kw; 3) Argon flow rate: Plasma: 1.4 l/min; 4) Auxiliary pressure: 0 psig; Nebuliser pressure: 30 psig; 5) Laser: Nd-YAG; 6) Laser mode: Q-switched; 7) Laser Wavelength: 266 nm; 8) Output energy: 10±1 mJ; 9) Facular aperture: 515 μm; 10) Helium flow rate: 800 ml/min. 11) limit of detection: 0.001. The LA-ICP-AES was equipped with a Nd-YAG laser and an RF generator of 40.82 MHz and 1.1 kw. The Q-switched laser mode was used with a laser wavelength of 266nm and output energy of 10±1 mJ. The auxiliary gas pressure and nebulizer gas pressure are 0 psi and 30 psi, respectively. The Argon flow rate in the Plasma was 1.4 L/min. Helium was used as the carrier gas with a flow rate of 800mL/min. The detection limit was 0.001. Silica was used as an internal standard for minor and trace element analysis of silicate materials by LA-ICP system. For major element analysis, external standards were used for data calibration due to the different silica contents in samples and standards. The glass standards are Nist-610/616 glass from the National Institute of Standards and Technology, Corning-B/D glass from Corning Museum of Glass. The analysts often use silica as an internal standard as this can generate good results for the minor and trace elements when analysing silicate materials using an LA-ICP system, but for major elements (especially for those elements whose concentrations are higher than 5%), the method does not work very well, because of the different silica content in the samples and standards; as a result, we cannot obtain the real silica content of the samples. Thus, if no data calibration is carried out, the analytical precision can be strongly influenced by some uncontrolled factors, produced by the laser ablating process itself. Data calibration must be an indispensable step for quantitative analysis using LA-ICP-AES. A simple but useful strategy is proposed in this paper. Calibration process includes: first, one external standard is used to get relative values of each element, then all results are summed up, and then the total is divided by each value to get the exact composition of each specimen. After calibrated, for homogenous material such as glass, after calibration, the relative standard deviations were mostly <1% for major

elements and <5% for minor and trace elements. The data recoveries were commonly 100±5% for major elements and 100±20% for minor and trace elements. Table 3 shows the normalized major element contents of the glass standards.

Table 2 Normalized major element contents of the glass standards

	Na_2O	MgO	Al_2O_3	SiO_2	P_2O_5	K_2O	CaO	TiO_2	Fe_2O_3	BaO	PbO
ɟB-	13.519	1.922	5.045	63.759	0.864	1.055	8.858	0.097	0.373	0.114	0.645
ɟB-	15.818	0.887	4.707	62.286	0.739	1.031	8.636	0.100	0.363	0.167	0.629
ɟB-	17.960	0.572	4.144	62.404	0.826	0.976	8.534	0.082	0.324	0.145	0.601
e	15.766	1.127	4.632	62.816	0.810	1.021	8.676	0.093	0.353	0.142	0.625
	2.221	0.706	0.455	0.819	0.064	0.041	0.166	0.010	0.026	0.027	0.022
	14.000	63.000	10.000	1.000	8.000	4.000	2.000	10.000	7.000	19.000	4.000
ɟC-	2.263	3.737	0.597	34.363	0.169	2.372	4.370	0.527	0.288	16.370	33.151
ɟC-	1.873	0.836	0.463	37.026	0.154	2.416	4.675	0.706	0.291	14.195	35.544
ɟC-	0.530	2.822	1.161	35.749	0.115	3.092	5.312	0.922	0.364	10.844	37.227
e	1.555	2.465	0.740	35.713	0.146	2.627	4.786	0.718	0.314	13.803	35.307
	0.909	1.483	0.370	1.332	0.028	0.404	0.481	0.198	0.043	2.784	2.048
	58.000	60.000	50.000	4.000	19.000	15.000	10.000	28.000	14.000	20.000	6.000
ɟD-	0.606	4.227	4.994	55.376	6.070	12.814	13.732	0.322	0.441	0.135	0.404
ɟD-	2.370	5.279	4.933	53.527	5.853	12.426	13.428	0.302	0.429	0.189	0.399
ɟD-	0.478	4.959	5.205	54.885	5.661	12.697	13.548	0.320	0.440	0.156	0.394
e	1.151	4.822	5.044	54.596	5.861	12.646	13.569	0.315	0.437	0.160	0.399
	1.057	0.539	0.143	0.958	0.205	0.199	0.153	0.011	0.007	0.027	0.005
	91.840	11.180	2.830	1.750	3.500	1.570	1.130	3.500	1.520	17.000	1.250

Table 3 Normalized major element contents of the glass standards.

	Na_2O	Mg_2O	Al_2O_3	SiO_2	P_2O_5	K_2O	CaO	TiO_2	Fe_2O_3
nist610	13.02656	0.09462	2.232313	71.5616	0.072804	0	11.91928	0.085487	0.09259
	13.12866	0.088105	2.20031	71.62484	0.084793	0	11.75111	0.081481	0.083137
	13.14144	0.088647	2.190642	71.64721	0.058638	0	11.8176	0.081058	0.081403
average	**13.099**	**0.090**	**2.208**	**71.611**	**0.072**	**0.000**	**11.829**	**0.083**	**0.086**
STD.	0.062961	0.003615	0.02181	0.044398	0.013093	0	0.084699	0.002444	0.006021
RSD.	0.48	4.00	0.99	0.06	18.16	0.00	0.72	2.96	7.02
	Na_2O	Mg_2O	Al_2O_3	SiO_2	P_2O_5	K_2O	CaO	TiO_2	Fe_2O_3
nist616	13.77148	0.057771	2.036412	70.02897	0	0	12.99668	0.591299	0.086656
	13.03738	0.015592	1.922014	72.68217	0	0	12.05936	0.036853	0.017009
	13.07011	0.016335	1.978835	72.70468	0	0	12.09469	0.022169	0.017501
average	**13.293**	**0.030**	**1.979**	**71.805**	**0.000**	**0.000**	**12.384**	**0.217**	**0.040**
STD.	0.41471	0.02414	0.0572	1.538366	0	0	0.531254	0.324432	0.040069
RSD.	3.12	80.74	2.89	2.14	0.00	0.00	4.29	149.66	99.21
	Na_2O	Mg_2O	Al_2O_3	SiO_2	P_2O_5	K_2O	CaO	TiO_2	Fe_2O_3
corning-d	1.379335	3.99087	5.801545	54.08346	3.937442	12.18632	15.39088	0.431479	0.563231
	1.400346	3.952812	5.649382	53.81079	4.163607	12.66544	15.07624	0.40583	0.544091
	1.357394	4.014839	5.722618	54.05477	4.043334	12.36447	15.23862	0.406145	0.544927
average	**1.379**	**3.986**	**5.725**	**53.983**	**4.048**	**12.405**	**15.235**	**0.414**	**0.551**
STD.	0.021478	0.031279	0.076099	0.149832	0.113159	0.242169	0.157345	0.014719	0.010817
RSD.	1.56	0.78	1.33	0.28	2.80	1.95	1.03	3.55	1.96
	Na_2O	Mg_2O	Al_2O_3	SiO_2	P_2O_5	K_2O	CaO	TiO_2	Fe_2O_3
corning-b -	16.09818	1.059483	4.635362	62.58427	0.903725	0.968652	9.076272	0.115097	0.396773
	16.1727	1.059768	4.594953	62.73591	0.909872	0.94136	8.942593	0.10824	0.38376
	16.15677	1.060588	4.585888	62.70378	0.889525	0.926207	9.002123	0.108634	0.386566
average	**16.143**	**1.060**	**4.605**	**62.675**	**0.901**	**0.945**	**9.007**	**0.111**	**0.389**
STD.	0.039244	0.000574	0.02634	0.079905	0.010436	0.02151	0.066973	0.00385	0.006848
RSD.	0.24	0.05	0.57	0.13	1.16	2.28	0.74	3.48	1.76

Raman spectroscopy is a non-destructive method for analyzing the material structure and the chemical bonds and interactions within the material by obtaining the fingerprint frequency of samples without special requirements for samples. It was performed at the Emperor Qin Shihuang's Mausoleum Site Museum (Xi'an, Shaanxi) at room temperature, using a 514 nm Nd:YAG laser for the spectral range from 100 to 1000 cm^{-1}. A laser power of 10 mW was employed, and the acquisition time was 10s for each integration and accumulated 3 times. The attribution of the Raman signatures of crystalline phases was made by comparing with data presented in the literature.

3. Results

Chemical composition

Table 4 Major elements composition of the glass beads（wt.%）

Sample ID	SiO_2	Al_2O_3	Fe_2O_3	MgO	CaO	Na_2O	K_2O	MnO_2	P_2O_5	TiO_2	Sb_2O_3	Method	Weathering degree
HLB1-blue	46.14	9.34	3.20	2.34	15.99	7.76	6.50	0.29	4.16	0.61	0.15	LA-ICP-AES	unweathered
HLB1-yellow	63.96	6.69	0.86	3.57	5.11	3.79	5.44	0.07	0.64	0.26	0.06	LA-ICP-AES	weathered
HLB2-blue	66.40	8.12	1.86	2.65	6.27	3.76	4.97	0.15	2.93	0.52	0.06	LA-ICP-AES	weathered
HLB2-yellow	52.33	4.89	1.03	1.69	4.23	2.48	3.36	0.05	2.85	0.28	0.07	LA-ICP-AES	weathered
HLB3- blue	67.44	4.37	0.57	3.32	3.43	12.55	6.20	0.08	0.49	0.16	0.01	LA-ICP-AES	unweathered
HLB3-white1	72.54	4.81	1.77	2.39	7.51	2.29	5.30	0.32	0.29	0.36	1.35	LA-ICP-AES	weathered
HLB4-blue	75.74	3.08	0.44	2.29	2.13	9.82	5.18	0.05	0.25	0.11	0.00	LA-ICP-AES	unweathered
HLB4-yellow	66.89	4.82	0.50	3.05	3.43	8.57	7.11	0.14	0.40	0.18	0.01	LA-ICP-AES	unweathered
HLB5-black	87.32	3.03	1.69	0.56	1.85	1.00	1.84	1.25	0.29	0.22	0.05	LA-ICP-AES	highly weathered
HLB5-white	72.55	2.40	0.53	0.50	1.52	2.88	2.17	0.19	0.41	0.18	8.49	LA-ICP-AES	weathered
HLB6-blue	87.32	2.65	1.03	0.76	2.54	1.75	1.98	0.36	0.34	0.24	0.09	LA-ICP-AES	highly weathered
HLB6-white	70.20	2.40	0.48	0.74	2.55	5.75	2.75	0.76	0.35	0.14	8.15	LA-ICP-AES	unweathered
HLB7	91.72	1.27	0.74	0.88	2.70	0.16	1.45	0.07		0.10	0.05	ED-XRF	highly weathered
HLB8-yellow	67.60	4.60	1.06	2.52	2.83	8.64	5.95	0.13	0.36	0.19	0.00	LA-ICP-AES	unweathered
HLB8-blue	83.84	6.69	0.48	1.70	1.84	1.00	2.71	0.09	0.29	0.21	0.01	LA-ICP-AES	highly weathered
HLB9-black	72.34	6.86	0.74	0.42	2.15	3.05	5.45	0.22	2.93	0.69	0.59	LA-ICP-AES	weathered
HLB9-white1	74.27	2.55	0.37	0.55	3.57	5.94	2.30	0.73	0.26	0.12	3.40	LA-ICP-AES	unweathered
HLB10	68.17	6.77	2.36	3.42	7.02	5.49	4.62	0.68	0.26	0.24	0.00	LA-ICP-AES	unweathered
HLB-11	81.24	4.31	1.30	1.71	4.23	0.49	2.80	0.22	0.02	0.27	0.28	ED-XRF	highly weathered
HLB12-blue	66.32	4.99	0.48	4.06	3.38	12.91	6.05	0.08	0.39	0.16	0.00	LA-ICP-AES	unweathered
HLB12-black	14.62	1.74	1.24	3.69	6.66	3.06	2.23	44.77	8.48	0.23	2.63	LA-ICP-AES	unweathered
HLB12-pink	54.56	4.16	2.97	12.11	5.54	2.08	5.22	0.40	8.02	0.48	0.08	LA-ICP-AES	unweathered
HLB12-white1	44.02	3.01	1.87	2.43	6.40	2.64	2.69	5.38	7.69	0.27	1.55	LA-ICP-AES	unweathered
HLB12-white2	20.50	2.11	1.41	2.97	10.20	2.40	2.71	9.26	17.18	0.52	1.73	LA-ICP-AES	unweathered

Sample ID	CuO	PbO	CoO	BaO	SnO_2	SrO	ZnO	B_2O_3	V_2O_5	NiO	ZrO	Ag_2O	Method	
HLB1-blue	0.82	0.23	0.02	0.16	0.44	0.09	0.80	0.20	0.38	0.37	0.00	0.01	LA-ICP-AES	unweathered
HLB1-yellow	0.08	7.02	0.00	0.15	1.86	0.05	0.15	0.09	0.07	0.06	0.01	0.00	LA-ICP-AES	weathered
HLB2-blue	0.63	0.14	0.01	0.24	0.46	0.05	0.18	0.09	0.32	0.19	0.00	0.00	LA-ICP-AES	weathered
HLB2-yellow	0.43	20.03	0.00	0.41	5.43	0.08	0.10	0.06	0.10	0.07	0.00	0.03	LA-ICP-AES	weathered
HLB3- blue	1.03	0.00	0.00	0.09	0.04	0.05	0.01	0.10	0.02	0.04	0.00	0.00	LA-ICP-AES	unweathered
HLB3-white1	0.26	0.21	0.05	0.21	0.07	0.02	0.08	0.10	0.02	0.04	0.01	0.01	LA-ICP-AES	weathered
HLB4-blue	0.61	0.00	0.00	0.14	0.02	0.03	0.00	0.05	0.01	0.02	0.00	0.00	LA-ICP-AES	unweathered
HLB4-yellow	0.01	4.17	0.00	0.11	0.46	0.04	0.00	0.06	0.01	0.02	0.01	0.00	LA-ICP-AES	unweathered
HLB5-black	0.16	0.00	0.09	0.13	0.11	0.03	0.07	0.14	0.05	0.11	0.00	0.00	LA-ICP-AES	highly weathered
HLB5-white	0.08	7.11	0.00	0.01	0.40	0.01	0.12	0.21	0.08	0.16	0.00	0.00	LA-ICP-AES	weathered
HLB6-blue	0.15	0.06	0.08	0.03	0.13	0.02	0.15	0.15	0.05	0.11	0.00	0.01	LA-ICP-AES	highly weathered
HLB6-white	0.06	5.40	0.00	0.02	0.08	0.02	0.06	0.07	0.01	0.02	0.00	0.00	LA-ICP-AES	unweathered
HLB-7	0.01	0.07	0.01	0.69	0.05	0.02	0.01						ED-XRF	highly weathered
HLB8-yellow	0.09	5.00	0.00	0.11	0.76	0.03	0.01	0.07	0.01	0.03	0.01	0.00	LA-ICP-AES	unweathered
HLB8-blue	0.67	0.03	0.00	0.11	0.09	0.02	0.01	0.11	0.04	0.07	0.00	0.00	LA-ICP-AES	highly weathered
HLB9-black	0.94	0.09	0.00	0.03	0.97	0.02	0.72	0.73	0.36	0.68	0.00	0.00	LA-ICP-AES	weathered
HLB9-white1	0.04	5.60	0.00	0.03	0.06	0.03	0.06	0.07	0.01	0.02	0.00	0.01	LA-ICP-AES	unweathered
HLB10	0.09	0.00	0.00	0.16	0.19	0.05	0.02	0.11	0.19	0.16	0.00	0.01	LA-ICP-AES	unweathered
HLB-11	2.11	0.02	0.01	0.76	0.13	0.10	0.02						ED-XRF	highly weathered
HLB12-blue	0.88	0.00	0.00	0.08	0.02	0.06	0.00	0.08	0.01	0.02	0.01	0.00	LA-ICP-AES	unweathered
HLB12-black	0.27	9.72	0.07	0.07	0.04	0.07	0.27	0.07	0.03	0.04	0.00	0.00	LA-ICP-AES	unweathered
HLB12-pink	0.80	2.79	0.00	0.06	0.09	0.05	0.33	0.13	0.05	0.09	0.01	0.00	LA-ICP-AES	unweathered
HLB12-white1	0.10	21.46	0.01	0.05	0.07	0.08	0.16	0.07	0.02	0.03	0.00	0.00	LA-ICP-AES	unweathered
HLB12-white2	0.20	28.14	0.01	0.04	0.06	0.14	0.30	0.07	0.02	0.04	0.00	0.00	LA-ICP-AES	unweathered

The glass components of different colors were tested and the chemical compositions were given as oxides in Table 4. The low Na_2O contents in some samples are mainly influenced by the weathering layer. In general, ancient glass from the tomb usually has a weathering layer with unknown thickness. The non-renewability of cultural relics requires the use of non-destructive or small-invasive test method when analyzing the glass beads. In our study, we used LA-ICP-AES to obtain the chemical composition through multiple tests at different depths and we chose the better data that minimize the influence of the weathered layer for discussion.

Based on the chemical compositions, all the glass beads from the Bizili site are soda-lime glass but with differences in the fluxes. Soda concentrations range from 1% to 12% and the lime concentrations vary from 1% to 15%, due to weathering in different degrees. Four of the opaque glass eye beads (HLB-1, HLB-2, HLB-4, and HLB-8) are similar in chemical compositions, except that the contents of SnO_2 and PbO in the yellow eyeballs are significantly higher than those in the blue base beads.

Raman spectroscopy

As shown in Figure 2, eight out of ten glass eye beads (HLB-1 to HLB-6, HLB-8, and HLB-9) are opaque. Raman spectroscopy was used to identify the crystals structures responsible for the opacification of the glass without damaging the samples. Tests conducted in the Emperor Qin Shihuang's Mausoleum Site Museum only found peaks in HLB-4 and HLB-5, possibly due to the weathering layers. Additional tests conducted at the Northwestern Polytechnical University gave same results. The results are shown in Figures 3 and 4.

The results of Raman spectroscopy in the yellow eyeballs show peaks at 134 cm^{-1} and 322 cm^{-1}, similar to the peak of lead-tin yellow, a synthetic material that is widely used in glass-making to get yellow and opaque glass [16]. According to the structures and chemical compositions, the lead-tin yellow has two types as Pb_2SnO_4 and $PbSn_{1-x}Si_xO_3$. Compared with the literature [17], the opacifier of the yellow eyeballs is $PbSn_{1-x}Si_xO_3$.

Four beads among the opaque beads (HLB-3, HLB-5, HLB-6, and HLB-9) show high contents of antimony ranging from 1.3 % to 8.1 % in the white parts, all tested by Raman spectroscopy. Only the surface was analyzed to avoid damage to the sample. Only HLB-5 shows a couple of peaks of different intensities at 232 cm-1 and 667 cm-1, corresponding to calcium antimonite ($Ca_2Sb_2O_6$) [14].

Microscopic observation

Although the number of samples from Bizili is limited, the glass beads are rich in manufacturing processes. We found three special types of glass beads, i.e. the glass eye beads, the etched beads and the glass beads with pigments. Figures. 5–7 show the microscopic observation of representative glass beads from different groups. The optical microscope can reveal the machining traces on the surface of glass beads, while SR-μCT can reveal the internal structures.

The etched glass bead HLB-10 is fragmentary. Its yellow band decoration could be observed under the microscope as shown in Fig. 6a. Figs. 6b and 6c show the SR-μCT of the body and the decoration, respectively.

Figure 7 shows the decoration of the glass bead with pigments under the microscope.

4. Discussion

4.1 Chemical compositions

The plot of MgO versus K_2O of the glass beads shows two distinctive groups. The first group (HLB-5, HLB-6, HLB-7 and HLB-9) with low MgO and K_2O contents could be considered as natron glass but with low Na_2O, which was possibly influenced by weathering. The natron glass is the predominant type of ancient glass in the Mediterranean and Europe from the middle of the 1st millennium B.C. until the 9th century A.D. [18][19]. Based on the research of Brill [26], these four samples are similar to the European glass in chemical composition. For example, the glass from Cosa (Roman) has MgO of 0.64%, K_2O of 1.12%, and Al_2O_3 of 2.43%, which are almost the same with our samples. In addition, the HLB-9 black has high contents of K_2O (5.45%) and Al_2O_3 (6.84%), possibly caused by the

use of impure sand or raw materials. Further research is needed to investigate the cause. HLB-5, HLB-6, and HLB-9 use white opaque glass as the base beads with different-colored eyeballs. The Fe_2O_3 contents in the black eyeballs are higher than that in the white base, making them appear black. The blue eyeballs mainly use Co as a coloring agent. Notably, HLB-7 has high transparency without perforation, which is possibly a semi-finished glass product.

The second group beads (HLB-1, HLB-2, HLB-3, HLB-4, HLB-8, HLB-10, HLB-11, and HLB-12) are characterized by high levels of both MgO and K_2O (over 1.5 wt.%). Brill suggested the MgO and K_2O contents above 1.5 wt.% indicated the use of plant ash during manufacturing [20]. Plant ash is quite variable in chemical composition because of different species of plants, growing environment, the plant parts used, and the burning temperatures [21]. Thus, the chemical compositions of plant ash glass vary slightly from region to region. The eight plant ash glass beads from the Bizili site might be from different regions. Five samples (HLB-1, HLB-2, HLB-4, HLB-8, and Hlb-10) are vegetable soda-lime glass (v-Na-Al glass) with high Al_2O_3. This type of glass has high Al_2O_3 over 4%, and MgO and K_2O higher than 1.5%. Dussubieux L [22] identified three main types of v-Na-Al glass. The first type was likely produced in Bara, Pakistan, a site dating from 200 B.C. to 200 A.D., and they are mainly glass ornaments found in North India, China (Xinjiang) and Bangladesh [23]. The other two types of v-Na-Al glass appear at younger sites dated from 900 A.D. and onward. Considering the spatial and temporal distribution of the v-Na-Al glass, our samples probably originated from Bara. The high contents of Al_2O_3 probably indicate the use of sand during production. Four of the five glass beads have similar appearance that comprises of blue glass base bead and yellow eyeballs with red and black glass concentric ornamentation made by different techniques. This special type of glass eye beads is found in large quantity in Bara and named as the Bara-type beads [2][10]. In terms of chemical composition, the Bara beads are soda-based and characterized by relatively high Al_2O_3 with CaO varying from 4.4 to 9.4%[24], similar to our samples. Collectively, the appearance, chemical compositions and distribution characteristics all suggest our glass bead samples originated from Bara.

We undertook comparative studies of other glass from literature to investigate if their compositions are representative of the glass from Central Asia, India and Mediterranean of the contemporary period. Some scholars considered potash and aluminum are very useful indicators in distinguishing plant ash glass from different origins [17]. In general, most plant ash glass production with K_2O higher than 4% suggests an origin from Central Asia, otherwise it might be from Western Asia. From the research of Brill [26], a plot of Al_2O_3 versus K_2O shows distinctive groups of beads from Mesopotamian, Indian, and Afghanistan. As shown in picture 9, both HLB-3, HLB-11 and HLB-12 fall into the Afghanistan origin, suggesting that they probably originated from Central Asia.

4.2 Opacifiers

Ancient craftsmen obtained opaque glass by adding opacifiers. Glass opacification process is often characterized by significant amounts of particles dispersed into glassy matrices. These particles include tin oxide, lead oxide, calcium antimonite, lead antimonite, etc[27]. The opaque glass beads from the Bizili site have antimony-based and tin-based opacifiers, of which the former was used earlier than the latter in glass production.

The antimony-based opacifiers were used in Egypt and the Near East in opaque glass production in the mid-second millennium B.C. [28], including lead-antimony oxide yellow and calcium antimony oxide white, until about the fourth century A.D.

Compared with antimony-based opacifiers, the tin-based opacifiers appeared later during the first to second centuries B.C.. The lead-tin oxide yellow glass appeared in Northwestern Europe, but the tin oxide white glass in this period is rare [27]. In about the fourth century, lead-tin oxide yellow glass was used in the Eastern Mediterranean and Levant and became an important part of glass making. During the early Islamic period (the eighth century), lead-tin oxide glass continued as shown in a set of glass tesserae. However, in the later Islamic period (ninth to tenth centuries), the tin oxide was more commonly used in Iraq and Iran [29-30]. The latest research tested lead stannate in a glass bead from Sardis (the eighth to the seventh century B.C.), which is the earliest known occurrence of tin-based opacifiers so far [31].

The lead-tin yellow exists as Pb_2SnO_4 or PbSn1-xSixO3, both with high refractive indices (> 2) [32]. During the production process of lead-tin yellow glass, the lead-tin calx, the fine powder that is left after heating a mixture of lead and tin to their melting point and beyond to temperatures above 600 °C is very important. The typical opaque yellow glass has a median Pb/Sn value of 9.1 [27]. In this study, except for HLB-4 with a Pb/Sn value of 9.07, the other three glass beads have relatively low Pb/Sn values (HLB-1=3.79; HLB-2=3.70; HLB-8=6.60).

The use of opacifiers was not a common feature of glass-making in Ancient China, because antimony-based opacifiers and tin-based opacifiers were not found in lead-barium glass, potassium glass or high-lead glass made in China. Thus, the opaque glass beads from the Bizili site were imported glass products. As the glass spread eastward, the use of opacifiers also gradually affected other areas. The glass beads produced at the Bara site were likely influenced by the West.

4.3 Manufacturing technology of glass beads

4.3.1 The glass eye bead

The Bara-type glass eye beads and other glass eye beads show obvious differences. The Bara-type glass eye beads share similar appearances and chemical compositions but are of low quality. Eyeballs are not bonded closely to the base beads and often fall off (Fig. 5b). Comparatively, other glass eye beads are well-made, and they look the same with the layered glass eye beads which were prevalent in the Mediterranean from the 6th to 3rd centruies B.C. In 1500 B.C., faience with similar appearance appeared in Egypt [33] and then gradually spread to Persia, South Russia, Central Europe and other regions [34][35]. During the East Zhou Dynasty (770 B.C.–256 B.C.), glass production and the glass-making technique have spread into China. Compared with glass vessels, the technique of making a glass bead is simpler, so the early glass products in China are mainly glass beads. Available archaeological records show a large number of similar glass beads found in southern China [36]. These glass beads are mainly lead barium glass that is uniquely made in China in addition to natron glass. The development of

China's early glass industry was likely influenced by layered glass beads. The craftsmen learned the glass bead manufacturing techniques and imitated the appearance of layered glass beads with local raw materials.

The microscopic features of glass eye beads shown in Fig. 10 indicate two ways to make eyeballs. In Fig. 10a, it is clear that the decoration is formed by overlapping glass of different colors from the top to the bottom. The manufacturers firstly obtained glass wafers with concentric circles by dropping glass liquid of different colors in sequence (Fig. 10b) as shown by the traces of glass flowing, and then inserted them into the base beads. The other method used a glass rod to dip glass liquid of different colors in sequence to produce concentric circles. When it was solidified, the rod was cut into blocks of suitable sizes and embedded into the base beads (Fig. 10a).

The variation of brightness on a CT slice reflects the differences in density and chemical composition, so the base beads and eyeballs can be clearly distinguished by different brightness. In general, air bubbles in glass were standard spherical shapes during the vitrifying process [37]. In Fig. 5e, a lot of air bubbles of different shapes spread across the base beads. Between the base beads and the eyeballs where the bubbles accumulated, the air bubbles are oblate and bigger than elsewhere. It indicates while the base beads were in a molten state, the craftsmen inserted the pre-made eyeballs into the base beads. Between the base beads and the eyeballs, the air bubbles were deformed by external pressure. As shown in Fig. 5e, the arrows indicate the pressure direction of inserting eyeballs into the base beads. Many small air bubbles fused here to form a bigger bubble. This provides further evidence that the base beads and eyeballs were separately made.

We drew a three-dimensional model based on the SR-uCT data of sample HLB-1 as shown in Fig 11 to identify how the glass beads were made.

In general, the ancient craftsmen mainly made glass beads by winding and drawing [38], normally, the bubbles in glass matrices were formed into standard spherical shapes during the vitrifying process [37]. However, the slender bubbles parallel to the perforation in Fig11 B indicate that the glass bead was made by drawing. Ancient manufacturers used tools called Lada, a long hollow metal pipe, in conjunction with a mobile inner rod known as the chetak [39] to draw glass into glass tubes, and then cut it into glass beads. Slender bubbles are the main feature of glass beads made by drawing. Figures11 C and11 D are enlargement of bubbles revealing more details. The shape of bubble in Fig11 D is different from others with an ellipsoid at one end. In the glass beads making process, the shape of bubble changed a lot by the influence of pull (the arrow represents the direction of the pull).

Table.5 The information of the sites

Site	Age
Jierzankale	600 B.C.–400 B.C.
Shanpula	100 B.C.–400 A.D.
Niya	202 B.C.–420 A.D
Bizili	202 B.C.–8 A.D.

In addition to the Bizili site, the Bara-type glass beads were found in many other sites of Xinjiang, including the Shanpula site [8], the Niya site [10], and the Jierzankale site [11]. Table 5 lists the details of the archaeological sites with the Bara-type glass beads in Xinjiang. From Table 5, except for the Jierzankale site, other sites correspond to the age of the Bara site (2nd B.C. to the 2nd A.D.). In addition, these sites, except for the Jierzankale site, have also excavated bi-color glass beads made of blue ground embedded with yellow curved stripes [37], which originated from Bara as well. These suggest the Bara-type glass eye beads from the Shanpula site, the Niya site, and the Bizili site may originate from the Bara site. Archaeological dating results show the lower age limit of the Jierzankale site is obviously earlier than the age of the Bara site, indicating the glass beads of blue monochrome base decorated with multi-color eyes were not created by Bara. The Bara site was probably influenced by other neighboring glass-making sites.

4.3.2 The etched glass bead

As shown in Fig.6, though the bead HLB-10 is fragmentary, the yellow band decorations could still be observed under the microscope. Fig. 6a clearly shows the position of the decoration, while Figs. 6b and 6c show many differences between the body and decoration on the SR-μCT. In Fig. 6b, the body is dense with scattered round air bubbles. The consistent brightness reflects a uniform glass phase in chemical composition. Comparatively, contrasting brightness exists in Fig. 6c. The inner part of the glass bead is brighter and dense with few bubbles, whereas the surface of the glass bead is darker and the structure is loose and porous with a large number of bubbles. The cause for this phenomenon is likely related to the manufacturing technology that used the same method with the etched carnelian bead, which originated in the Indus Civilization. The etched carnelian beads were found at the Chanhu-Daro site of the Harappa Culture in the Indus Valley at first. The craftsmen firstly mixed a special plant juice with alkali, then etched out patterns on the base bead, and buried the beads in charcoal ash for permanent decoration. A large number of etched carnelian beads have been excavated in India and they display different patterns of decoration, including the cruciform ornament [40]. According to the SR-μCT results, the etched glass bead in this study was probably made by the same process as the etched carnelian bead was. The decoration area has a lot of bubbles because of chemical reactions between glass and alkali. The alkali solution penetrates downward, causing the corrosion layer. It is likely a new type of glass bead influenced by the etched carnelian beads. Both studies on chemical composition and the manufacturing technology indicate the etched glass beads from the Bizili site probably originated from India.

4.3.3 The glass bead with pigment

The glass beads with pigment (HLB-12) have blue base beads with eye-like decorations. According to the results of LA-ICP-AES, the base bead is plant ash soda-lime glass, though the content of SiO_2 in the decoration area is very low. The black area is high in MnO_2 (44.7%) and the white area contains 21.4%−28.1% of PbO, indicating that the material used on the surface was probably inorganic mineral pigments rather than glass. From optical observations, the pigment layer is very thin, and less than one millimeter with a lot of particles. In the process of making glass beads, the craftsmen fused the monochromatic glass to make the base beads and then drew different ornamentations on the base beads with pigments of different colors. To combine the base beads and the pigments, these glass beads were probably fired again. When the temperature is high, the decorations may become less regular due to the fluidity of glass.

The glass beads with pigment are rarely found in archaeological excavations except in China. Based on archaeological reports [15, 41], using pigments to decorate glass beads has already appeared in Central Plains (China) during the Warring States period. The features of chemical composition of HLB-12 correspond to Central Asia, suggesting such decorating method probably appeared in Central Asia in the Western Han dynasty. Given that the technology appeared earlier in China than in Central Asia, we don't exclude the possibility that Central Asia was influenced by China.

5. Conclusion

The early glass production mainly occurred along the Tianshan Mountains in Xinjiang, related to the Mesopotamia and Europe. After the Western Han Dynasty, glass production along the south of the Silk Road grew explosively, and the impact of India had become manifest [42][43].

This study analyzed glass beads from the Bizili site located on the southern road of the Silk Road. They are all soda-lime glass and can be divided into natron glass and plant ash glass based on their fluxes. The comparative study on the chemical composition and appearance between the samples with glass beads from other regions show that they have strong foreign cultural characteristics that were believed to have originated from many regions. The natron glass is the predominant type of ancient glass in the Mediterranean and Europe and spread to China by the ancient nomadic people. The eight glass beads belong to the plant ash glass, originate from both Central Asian and Kushan (Bara site), with the latter mainly distributed on the southern limb of the oasis Silk Routes. Archaeological chronological evidence shows that the glass beads of blue monochrome base glass decorated with multi-color eyes were not created by Bara but was probably influenced by other neighboring glass-making sites. The opaque glass beads detected antimony-based and tin-based opacifiers, suggesting that they are exotic products. In terms of glass beads making technology, there are two ways to make eyeballs for glass eye beads of the Bara type, and the base beads were made by drawing. Meanwhile, new types of glass beads were discovered including the etched glass bead and the glass bead with pigments.

This research suggests that the Bizili site was influenced by many cultures, especially ancient India. With the opening of the Silk Road, the trade and the cultural exchange between various regions became more frequent, so

glass products appeared in large quantity during the Han dynasty.

Declarations

Availability of data and materials

Please contact the corresponding author upon reasonable data requests.

Abbreviations

SR-μCT: Synchrotron Radiation Microtomography

ED-XRF: Energy Dispersion X-ray Fluorescence Spectrometry

LA-ICP-AES: Laser Ablation Inductively-coupled Plasma Atomic Emission Spectroscopy.

Acknowledgment

This study was sponsored by the National Natural Science Foundation of China (Grant No. 11575142). Special thanks go to the Shanghai Synchrotron Radiation Facility for helping with the analysis and the Xinjiang Institute of Cultural Relics and Archaeology for providing the glass beads samples in this study. Thanks to Fengjian Cui for debugging instrument and calibration of LA-ICP-AES. Many thanks also to Xiaoya Zhan for modifying the language.

Authors' contributions

Dong Wang and Rui Wen designed the research described in this paper. All the experiment was done by Dong Wang. Dong Wang and Rui Wen drafted the majority of the manuscript. Xingjun Hu and Wenying Li provided the samples in this study. All authors have read and approved the final manuscript.

Ethics declarations

Ethics approval and consent to participate

This article does not contain any studies with human participants or animals performed by any of the authors.

Consent for publication

The consent for the publication of details and images in the manuscript are obtained from all participants.

Competing interests

The authors declare that there are no conflicts.

Funding

Beyond the National Natural Science Foundation of China (Grant No. 11575142) support, the school of cultural heritage, Northwest University also supported this research (2019WYYCY-04).

Publisher's Note

Springer Nature remains neutral with regard to jurisdictional claims in published maps and institutional affiliations.

Author information

Affiliations

Key Laboratory for Cultural Heritage Study & Conservation (Northwest University), Ministry of Education, Xi'an, China

Dong Wang, Rui Wen

Research Center for Archaeological Science, Northwest University, Xi'an, China

Dong Wang, Rui Wen

Xinjiang Institute of Cultural Relics and Archaeology, Urumchi, China

Xingjun HU c, Wenying Li

Corresponding author

Correspondence to Rui Wen.

References

1. Ge Chen. Study on the cultures of the Bronze Age and early Iron Age in Xinjiang area. Archaeology, 1990(4), 366-374 (In Chinese).
2. Liu, Q.H. Li, F. Gan, P. Zhang, J.W. Lankton, Silk Road glass in Xinjiang, China: chemical compositional analysis and interpretation using a high-resolution portable XRF spectrometer, Journal of Archaeological Science, 2012(7): 2128-2142.
3. Wang Yingzhu. The technological research of faience in Western Zhou and Eastern Zhou periods. University of science and technology Beijing, 2019 (In Chinese).

4. Lin Y, Rehren T, Wang H, et al. The beginning of faience in China: A review and new evidence. Journal of Archaeological Science, 2019, 105: 97-115.
5. Liu N, Yang Y, Wang Y, et al. Nondestructive characterization of ancient faience beads unearthed from Ya'er cemetery in Xinjiang, Early Iron Age China [J]. Ceramics International, 2017,43 (13):10460-10467.
6. Xinjiang Institute of Cultural Relics and Archaeology. Saensayi site of Xinjiang, China. Cultural Relics, 2013 (In Chinese).
7. Gan Fuxi, Li Qinghui, Gu Donghong, et al. Study on early glass beads unearthed from Baicheng and Tacheng of Xinjiang. Journal of The Chinese Ceramic Society, 2003(07):663-668.
8. Xinjiang Institute of Cultural Relics and Archaeology. Shanpula, Xinjiang, China. The Peoples Press of Xinjiang, 2001 (In Chinese).
9. Zhiyong Yu. Archaeological Excavation of Niya site M8 Cemetery in Xinjiang. Cultural relics, 2000(1):4-40 (In Chinese).
10. Yixian Lin. A scientific study of glass finds from the Niya site in Xinjiang (Doctoral dissertation). 2009 (In Chinese).
11. Xinhua Wu. Archaeological Excavation of Jierzankale Cemetery in Xinjiang in 2013. The Western Regions Studies, 2014(01):124-127(In Chinese).
12. Qian Cheng, Jinlong Guo, el all. Characteristics of chemical composition of glass finds from the qiemo tomb sites on the Silk Road. Spectroscopy and Spectral Analysis, 2012(07): 1955-1960.
13. Xingjun Hu et al. New Archaeological discovery of Bizili Cemetery in Luopu County, Xinjiang. The Western Regions Studies, 2017(01):144-146(In Chinese).
14. Ju Yang, Hongxia Zhao, Pu Yu. Analysis of composite glass beads (eye-beads) unearthed from the Shahe Tomb in the Changping District of Beijing. Sciences of Conservation and Archaeology, 2012, 24(02):74-83(In Chinese).
15. Deyun Zhao. Exotic Beads and Pendants in ancient China: From Western Zhou to Eastern Jin Dynasty. Science Press, 2016 (In Chinese).
16. Qian Cheng, Jinlong Guo. The Use of Antimony and Tin in Ancient Western Glass Making. Tenth National Symposium on Archaeology and Heritage Conservation, 2008(In Chinese).
17. Song Liu. The development of portable X-Ray fluorescence analysis and its application in scientific and technological archaeology. 2011(In Chinese).
18. Sayre, E.V., Smith, R.V. Compositional categories of ancient glass. Science, 1961 133(3467): 1824-182612
19. Gallo F, Silvestri A, Molin G. Glass from the Archaeological Museum of Adria (North-East Italy): new insights into Early Roman production technologies. Journal of Archaeological Science, 2013, 40(6):2589-2605.
20. BRILL R H. Chemical Analysis of Early Glasses [M]. New York: The CorningMuseum of Glass, 1999.
21. Oudah Y B, Henderson J. Plant Ashes from Syria and the Manufacture of Ancient Glass: Ethnographic and Scientific Aspects. Journal of Glass Studies, 2006, 48(1):297-321.
22. Dussubieux L, Gratuze B, Blet-Lemarquand M. Mineral soda alumina glass: occurrence and meaning. Journal of Archaeological Science, 2010, 37(7):0-1655.
23. Dussubieux, L., Gratuze, B.. Nature et origine des objets en verre retrouve´s a$Begram(Afghanis\tan)eta$ Bara (Pakistan). In: Bopearachchi, O., Landes, C.,Sachs, C. (Eds.), De l'Indus a` l'Oxus: Arche´ ologie de l'Asie Centrale. Association Imago, Muse´e de Lattes, Lattes, 2003: 315–323.

24. Dussubieux L, Bernard Gratuze. Glass in South Asia. In modern methods of analyzing archaeological and historical glass, K. Janssens (Ed.) 2013:401-430.
25. Brill R H. Opening Remarks and Setting the Stage: Lecture at the 2005 Shanghai International Workshop on the Archaeology of Glass along the Silk Road. Ancient Glass Research along the Silk Road. 2009: 109-147.
26. Brill R H. Chemical Analyses of Early Glasses. The corning museum of glass corning, New York. 1999:332-340.
27. Matin M. Tin-based opacifiers in archaeological glass and ceramic glazes: a review and new perspectives. Archaeological and Anthropological Sciences: 1-13.
28. Shortland A J. The use and origin of antimonate colorants in early Egyptian glass. Archaeometry, 2002, 44:517-530.
29. Fiorentino S, Vandini M, Chinni T, Caccia M, Martini M, Galli A. Colourants and opacifiers of mosaic glass tesserae from Khirbet al-Mafjar (Jericho, Palestine): addressing technological issues by a multi-analytical approach and evaluating the potentialities of thermo-luminescence and optically stimulated luminescence dating. J Archaeol Anthropol 2017:1–23.
30. Fiorentino S, Chinni T, Cirelli E, Arletti R, Conte S, Vandini M. Considering the effects of the Byzantine-Islamic transition: Umayyad glass tesserae and vessels from the qasr of Khirbet al-Mafjar (Jericho, Palestine). J Archaeol Anthropol. 2018(10):223–
31. Alicia Van Ham-Meert, Sarah Dillis,et al. A unique recipe for glass beads at Iron Age Sardis. Journal of Archaeological Science, 2019 (108): 0305-4403.
32. Clark, R.J.H.; Cridland,L.; Kariuki, B.M.; Harris, K.D.M.; Withnall, R. Synthesis, structural characterization and Raman spectroscopy of the inorganic pigments lead-tin yellow types I and II and lead antimonate yellow: Their identification on medieval paintings and manuscripts. Journal of the Chemical Society, Dalton Transactions, 1995(16), 2577-2582
33. Fuxi Gan. Development of Chinese Ancient Glass. Shanghai Scientific & Technical Publishers, 2016 (In Chinese).
34. SPARE M. Some observations on the stratified Mediterranean eye-beads of the first millennium BC. Association internationale pour l'historie du verre. Annales du 10e congres de l'association internationale pour l'histoire du verre 1985. Amsterdam: International Association for the History of Glass, 1987: 1-12.
35. SPARE M. Ancient glass in the Israel museum beads and other small objects. Jerusalem: The Israel Museum, 2001.
36. Yanjiao Yu. Research on Beads Unearthed from Hunan Province. Hunan people's publishing house, 2018 (In Chinese).
37. Cheng Qian, Zhang X, Guo J, et al. Application of computed tomography in the analysis of glass beads unearthed in Shanpula cemetery (Khotan), Xinjiang Uyghur Autonomous Region. Archaeological and Anthropological Sciences, 2017.
38. An jiayao. A brief history of glasswares in China. Beijing: Social Sciences Academic Press, 2011. (In Chinese).
39. Kanungo, A.K., 2001. Glass Beads in Indian Archaeology: An Ethnoarchaeological Approach. 60–61. Bulletin of the Deccan College, pp. 337–353.
40. Deyun Zhao. Study on Etched Carnelian Beads Unearthed in China. Archaeology, 2011(10):68-78 (In Chinese).
41. Xiaojuan Huang, Jing Yan, Hui Wang. Analysis of the Decorated Silicate beads Excavated from Tomb M4 of the Ma-Jia-Yuan Warring States Cemetery, Gansu Province. Spectroscopy and Spectral Analysis, 2015(10):2895-2900 (In Chinese).

42. Qian Cheng, Chun Yu, Lin Xi, Wei He. A Test and preliminary Study of the Composition of the Glass Excavated from the Norbutso Site of Ngari in Tibet-and a Discussion of the Silk Road in Ngari. Journal of Tibetology, 2017(02):264-274 (In Chinese).
43. Hongliang Lv. The study on the early burials in the western Himalaya region. Acta Archaeologica Sinica, 2015(01):1-34(In Chinese).

Figures

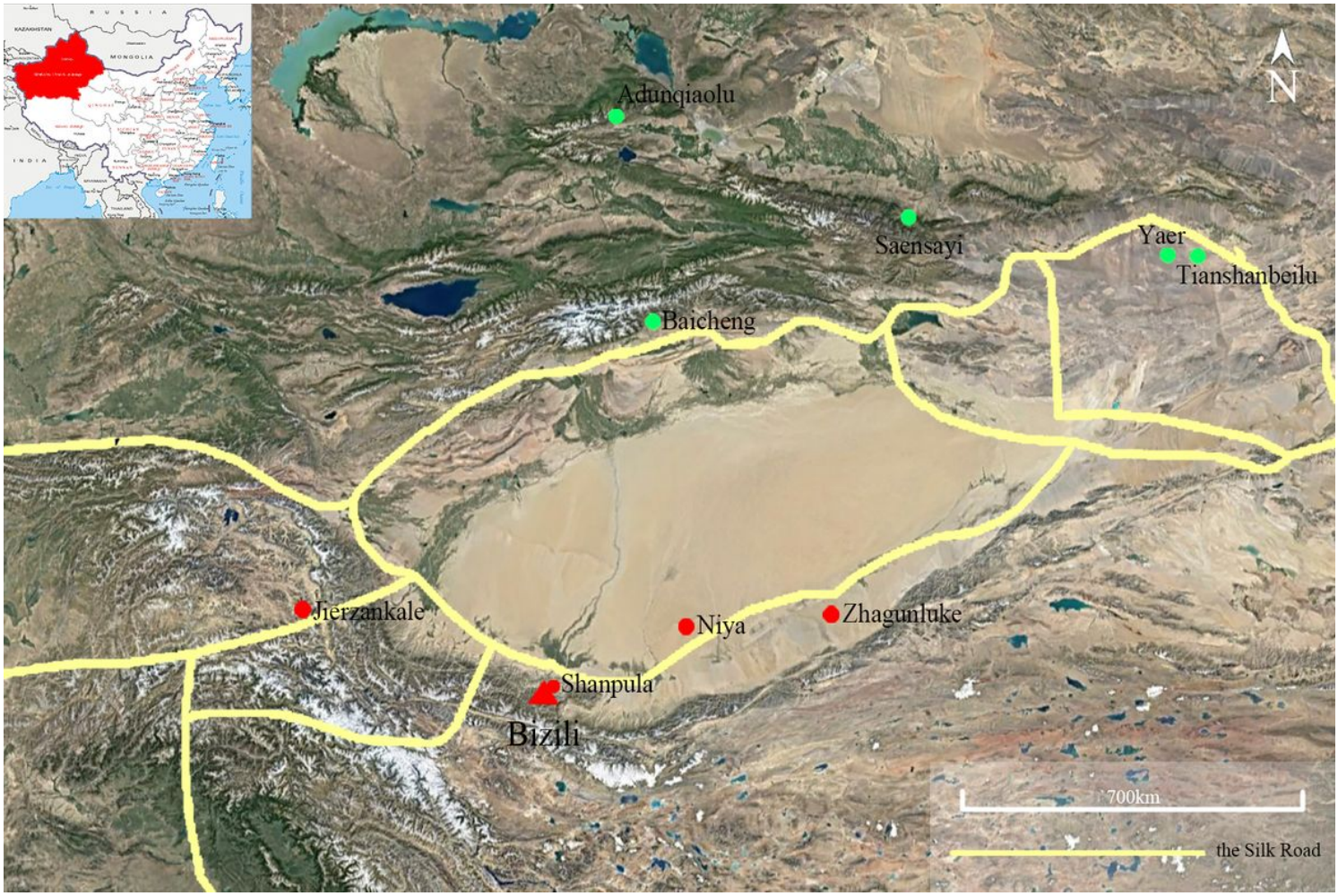

Figure 1

Map of Xinjiang. The Bizili site is labeled. Sites before 500 B.C. (green) and after 500 B.C. (red). Note: The designations employed and the presentation of the material on this map do not imply the expression of any opinion whatsoever on the part of Research Square concerning the legal status of any country, territory, city or area or of its authorities, or concerning the delimitation of its frontiers or boundaries. This map has been provided by the authors.

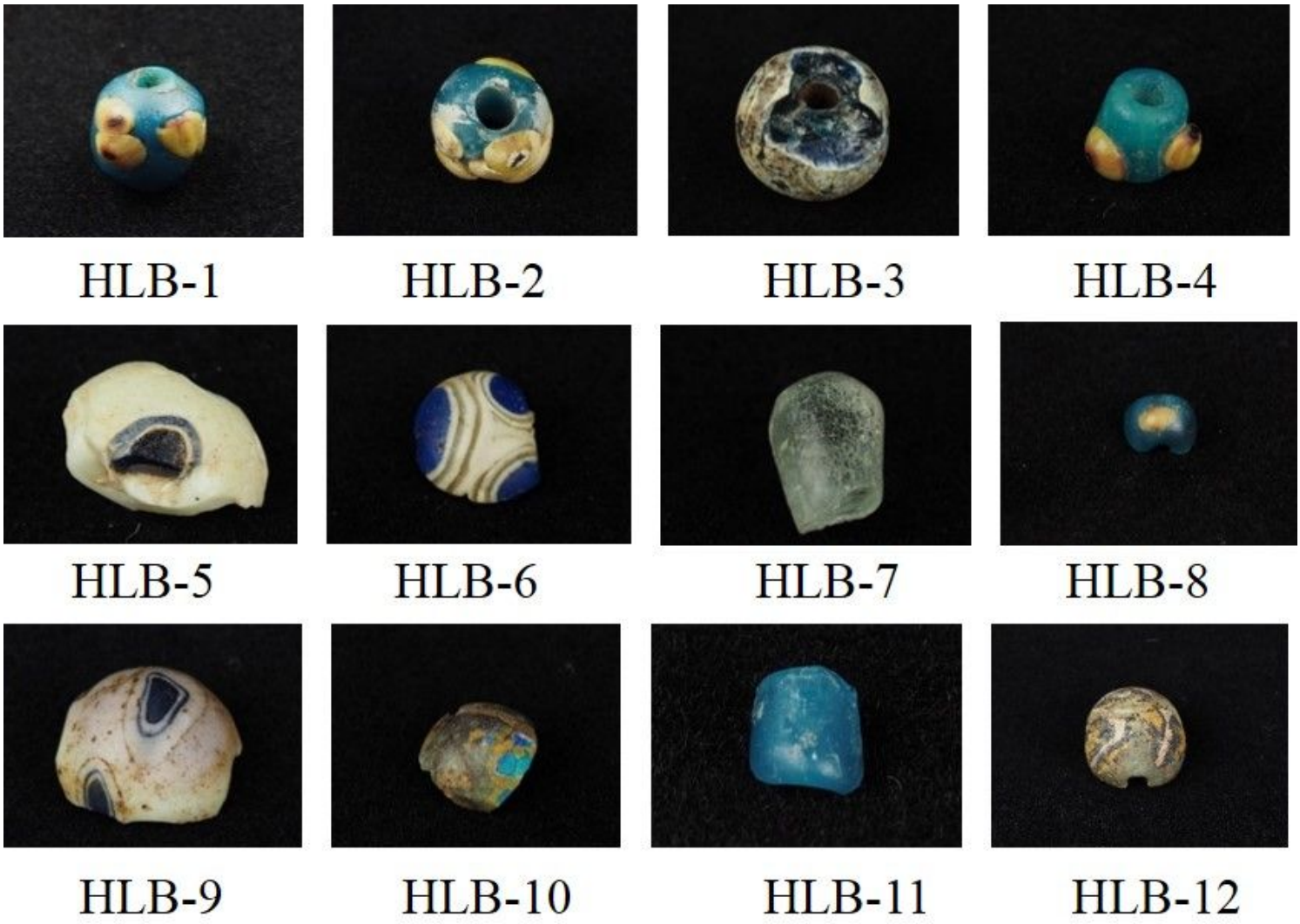

Figure 2

Ancient glass beads from the Bizili site in Xinjiang

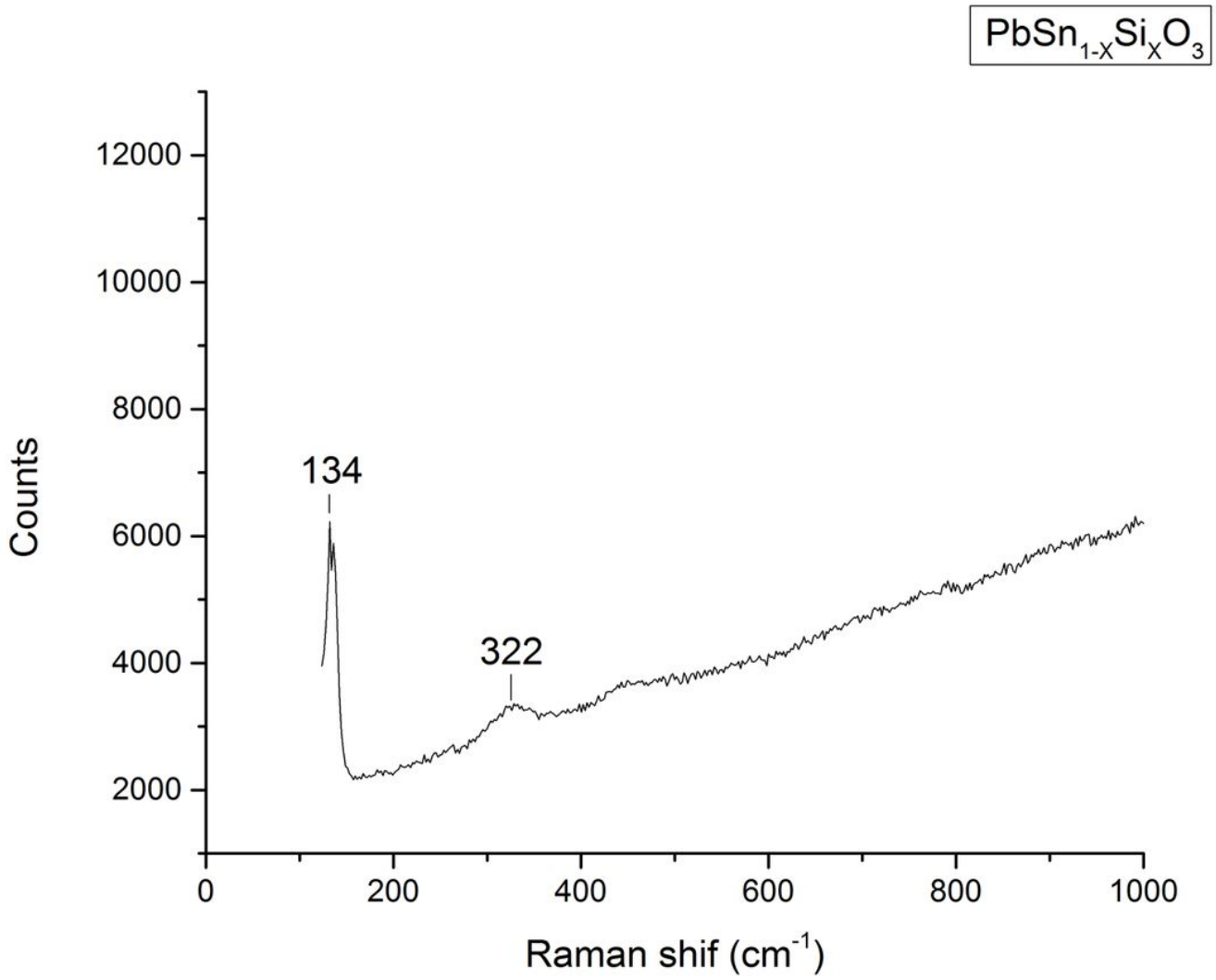

Figure 3

Raman spectroscopy analysis of sample HLB-4.

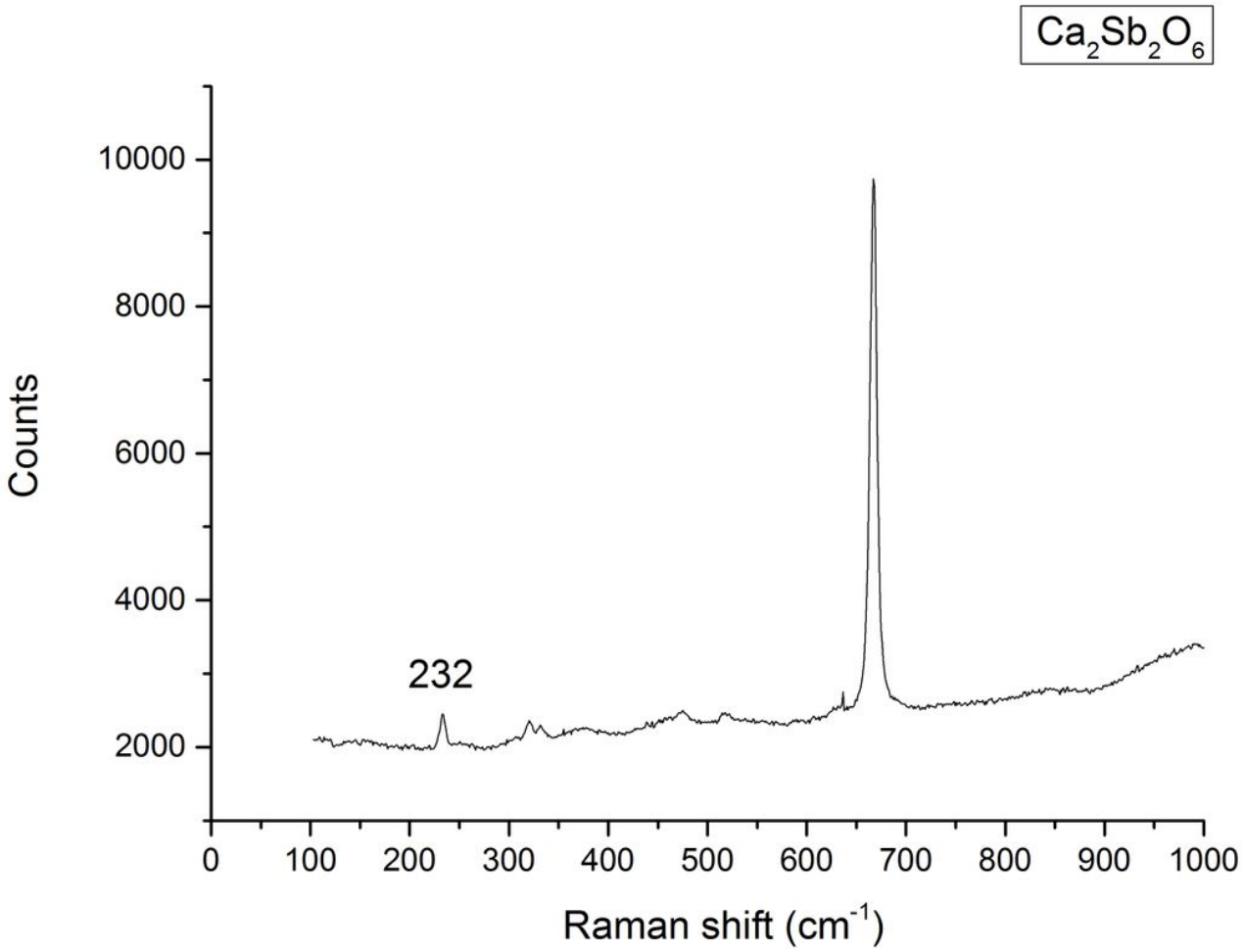

Figure 4

Raman spectroscopy analysis of sample (HLB-5).

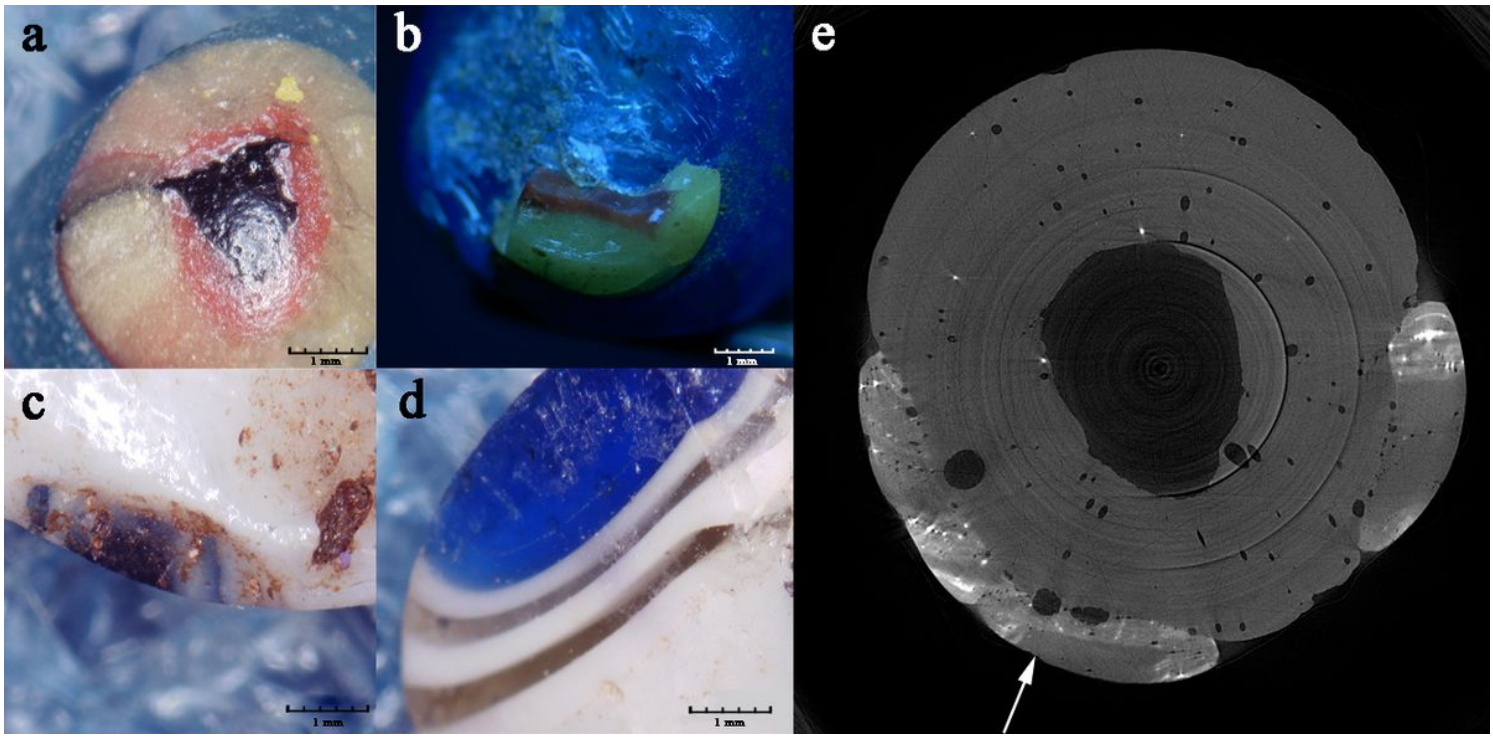

Figure 5

Microscopic observation of the glass eye beads (a: HLB-1; b: HLB-4; c: HLB-9; d: HLB-6; e: HLB-1)

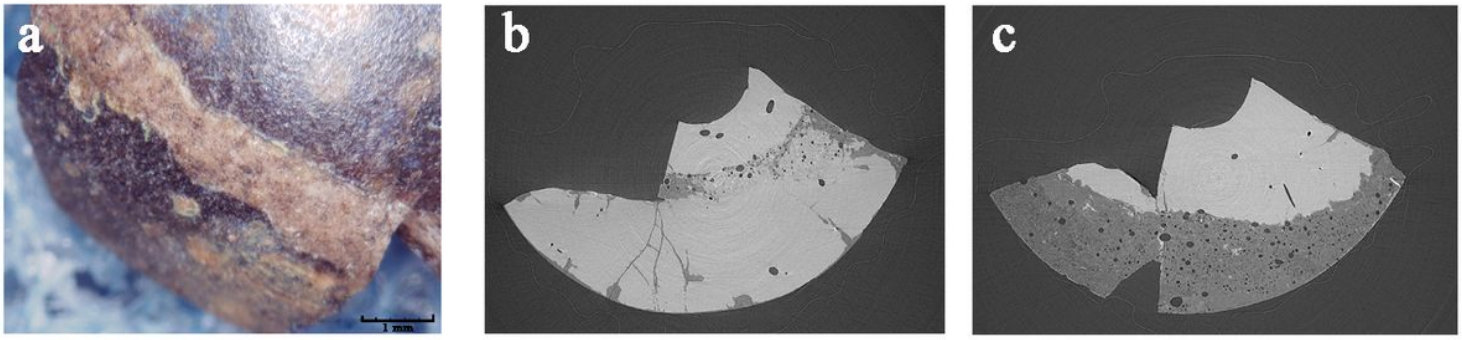

Figure 6

Microscopic observation of the etched glass bead (HLB-10)

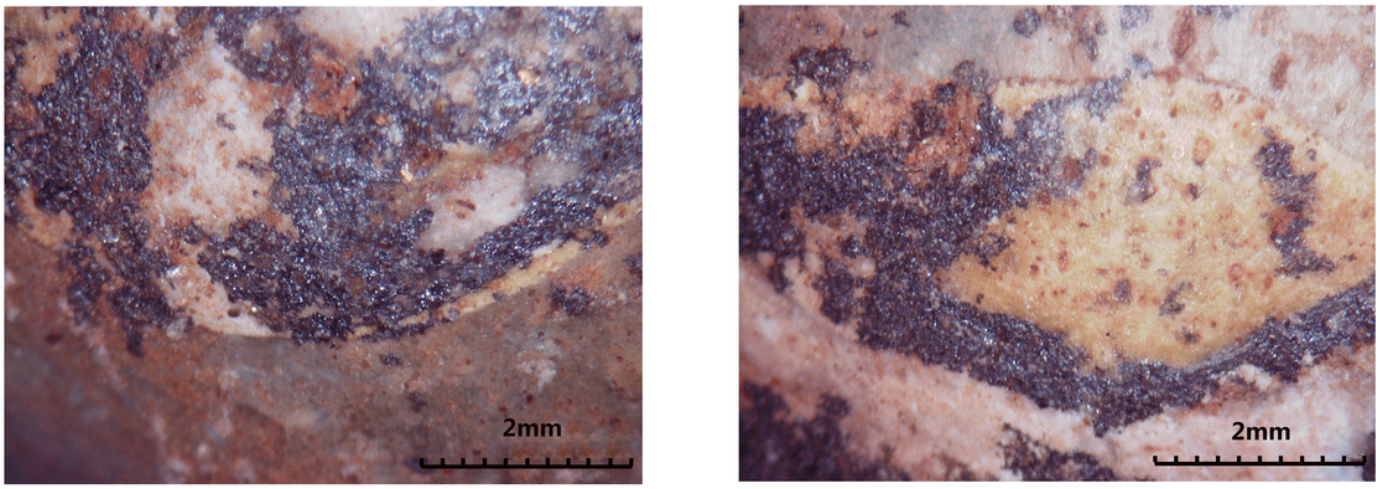

Figure 7

Microscopic observation of the glass bead with pigment (HLB-12)

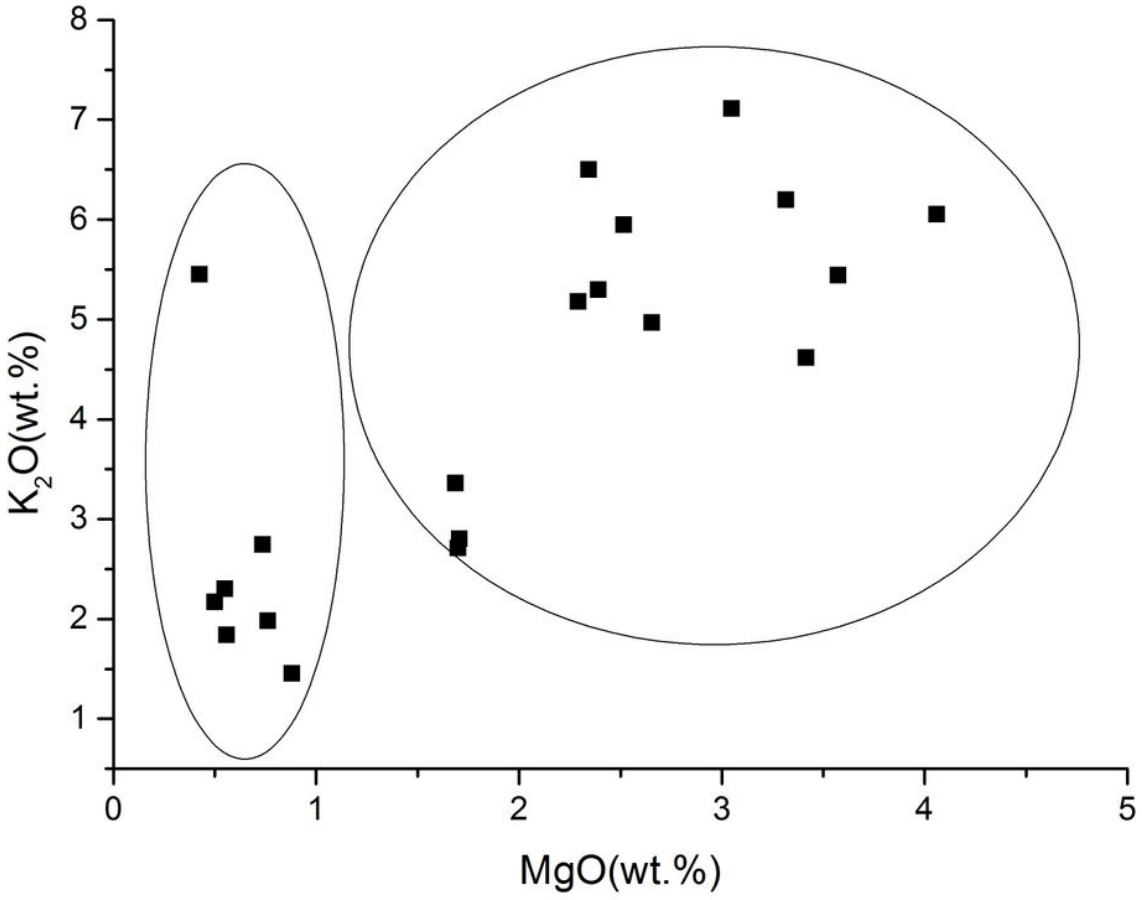

Figure 8

Plot of K2O/MgO.

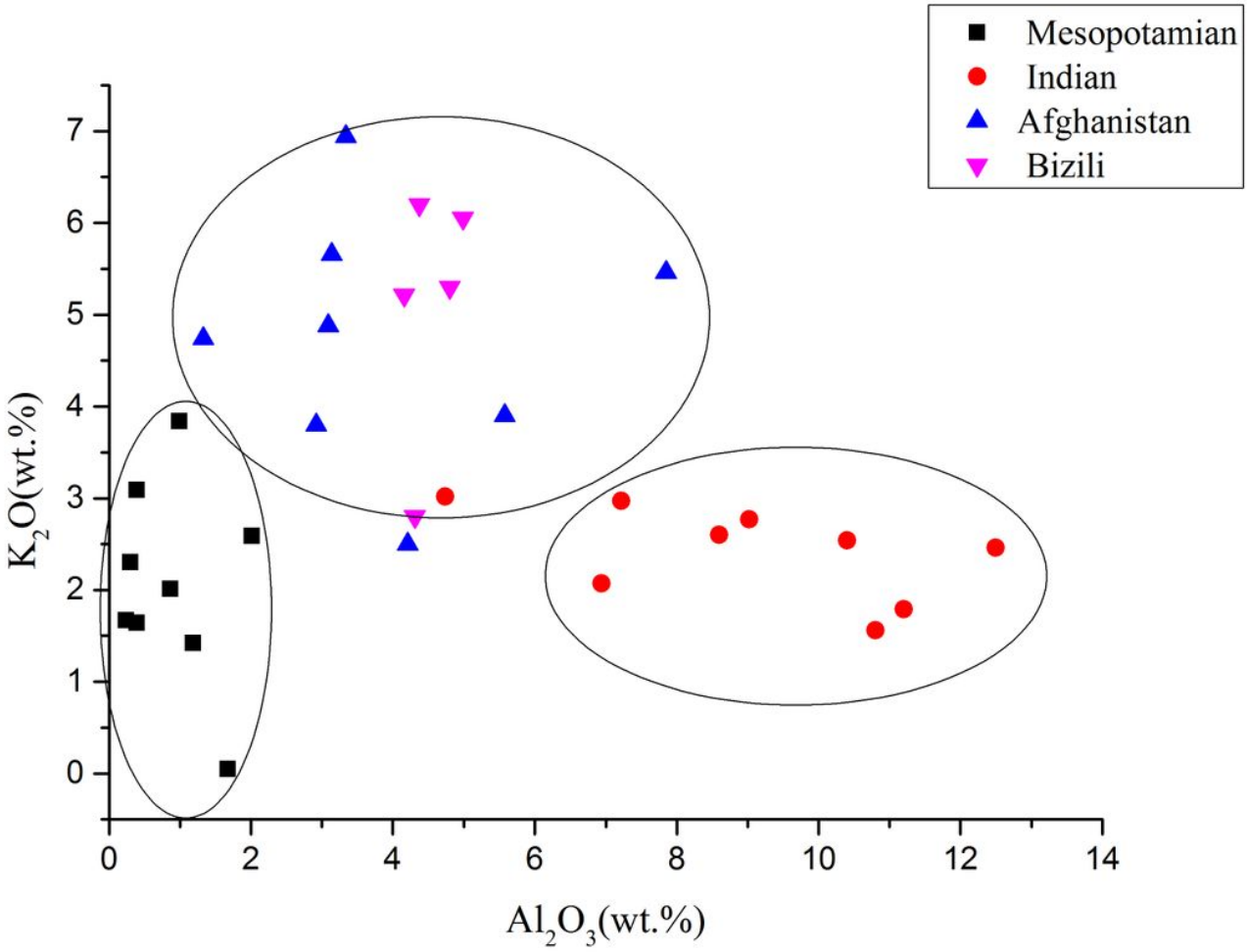

Figure 9

Plot of K2O / Al2O3.

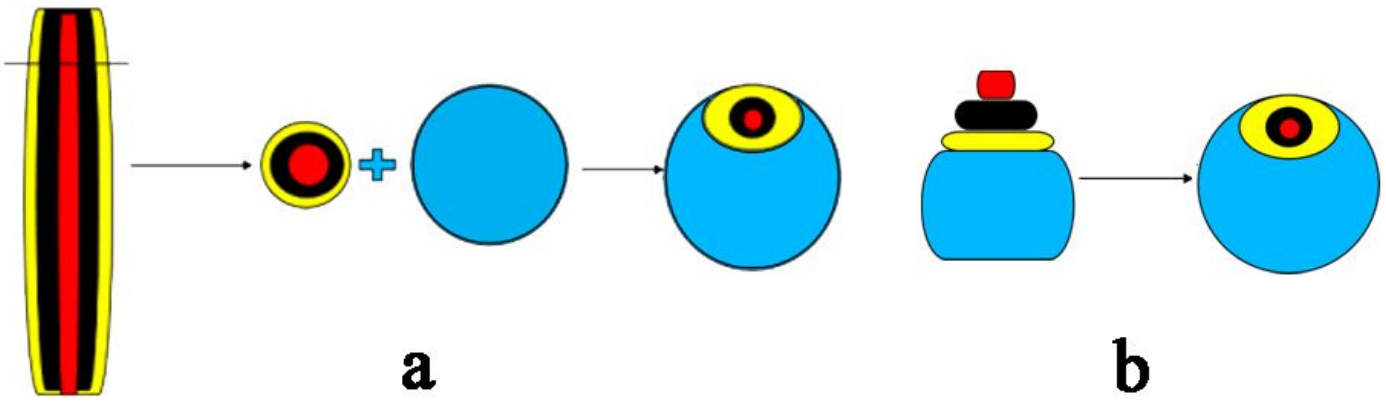

Figure 10

The manufacturing process of glass eye beads (HLB-1, HLB-2, HLB-4, HLB-8)

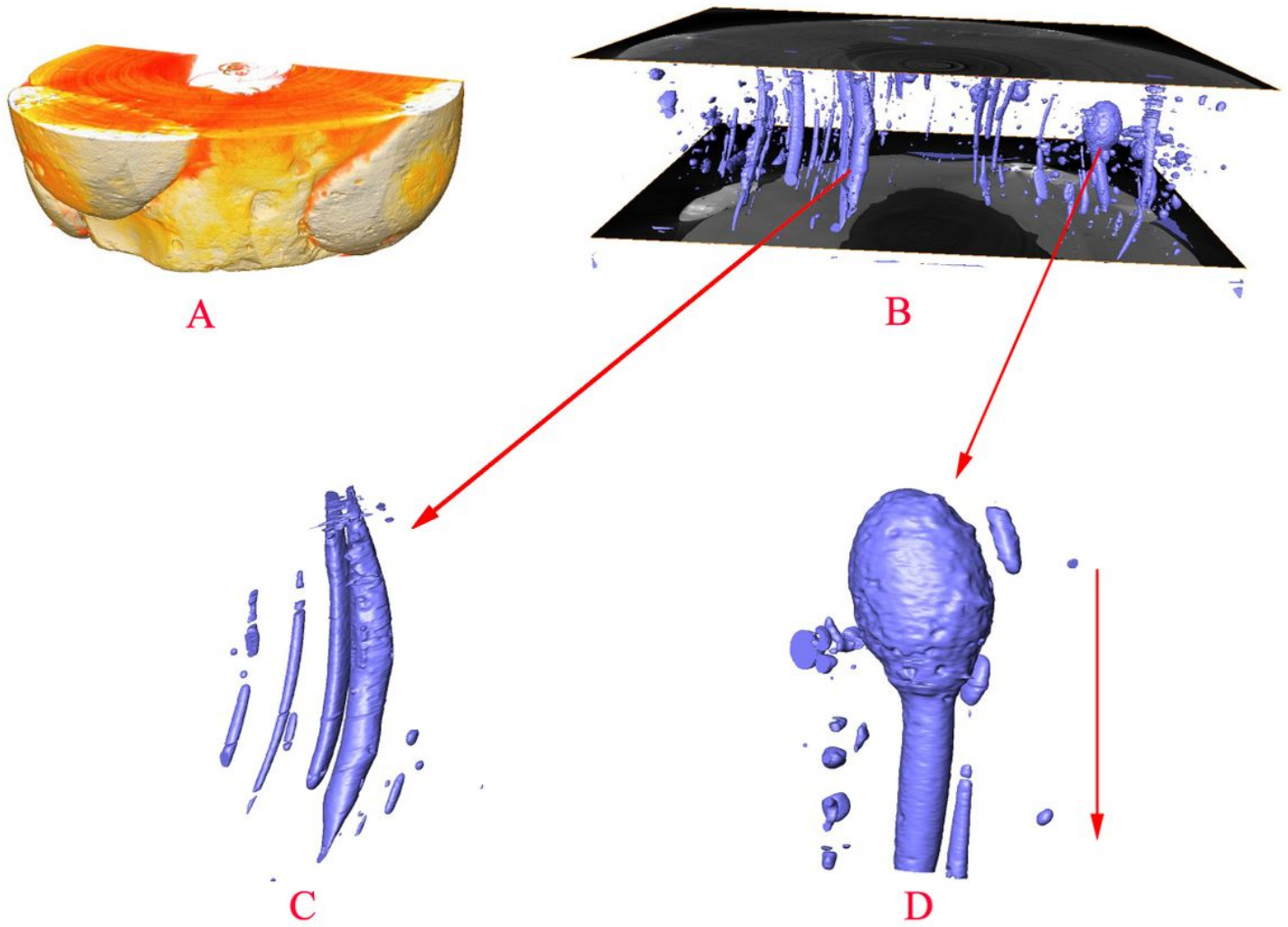

Figure 11

Three-dimensional model of sample HLB-1

Figure 12

Bara-type glass eye beads from other sites